available at www.sciencedirect.com

SCIENCE DIRECT®

journal homepage: www.elsevier.com/locate/biochempharm

Paradoxical effects of the phage display-derived peptide antagonist IGF-F1-1 on insulin-like growth factor-1 receptor signaling

Stephanie A. Robinson, Steven A. Rosenzweig *

Department of Cell and Molecular Pharmacology & Experimental Therapeutics and Hollings Cancer Center, Medical University of South Carolina, 173 Ashley Avenue, Charleston, SC 29425, United States

ARTICLE INFO

Article history:
Received 22 February 2006
Accepted 30 March 2006

Keywords:
Insulin-like growth factor-1
Insulin-like growth factor binding proteins
Insulin-like growth factor antagonist
Structure–function
Breast cancer

Abbreviations:
Akt, protein kinase B (PKB) alpha isoform
BCA, bicinchoninic acid
BLOTTO, bovine lacto transfer technique optimizer
BSA, bovine serum albumin
Erk, extracellular-signal-regulated kinase
FBS, fetal bovine serum
Flt-1, fms-like tyrosine kinase-1
HRP, horse radish peroxidase
IGF-1, insulin-like growth factor 1
IGF-1R, IGF-1 receptor
IGFBP, IGF binding protein
IP, immunoprecipitation
IB, immunoblot

ABSTRACT

The insulin-like growth factor binding proteins (IGFBPs) represent a unique class of IGF antagonists regulating the bioavailability of the IGFs extracellularly. Accordingly, they represent an important class of proteins for cancer therapeutics and chemoprevention. IGF-F1-1 is a cyclic hexadecapeptide identified by high throughput phage display that binds to the IGFBP-binding domain on IGF-1. It acts as an IGFBP-mimetic, capable of inhibiting IGF-1 binding to the IGFBPs. To further examine the utility of IGF-F1-1 as an IGF-1 antagonist we tested its ability to inhibit IGFBP-2 and IGFBP-3 binding to IGF-1, ^{125}I-IGF-1 binding to IGF-1Rs and to block IGF-1 induced Akt activation, cell cycle changes and [^{3}H]thymidine incorporation in MCF-7 cells. These biological activities were inhibited by treatment with IGFBP-2, wortmannin or the IGF-1R tyrosine kinase inhibitor, NVP-AEW541, but not by IGF-F1-1. Our findings confirm previous studies indicating that IGF-F1-1 is a weak antagonist of IGF-1 binding to the IGFBPs and the IGF-1R and suggest that it does not effectively inhibit downstream events stimulated by IGF-1. We further demonstrated that IGF-F1-1 treatment of MCF-7 cells results in the paradoxical activation of Akt, S-phase transition and [^{3}H]thymidine incorporation. These results suggest that IGF-F1-1 is a weak agonist, exhibiting mitogenic actions. IGF-F1-1 may act in conjunction with IGF-1 at the IGF-1R or independently of IGF-1 at the IGF-1R or another receptor.

* *Corresponding author*. Tel.: +1 843 792 5841; fax: +1 843 792 2475.
E-mail address: rosenzsa@musc.edu (S.A. Rosenzweig).
0006-2952/$ – see front matter
doi:10.1016/j.bcp.2006.03.025

MAPK, MEK/mitogen-activated protein kinase
PBS, phosphate-buffered saline
PI 3-K, phosphatidylinositol 3-kinase
TBS, Tris-buffered saline
WCE, whole cell extract

1. Introduction

The IGF-1R plays a crucial role in cell transformation and tumorigenesis [1], with numerous epidemiological studies indicating IGF-1 as a positive risk factor for the development of breast, prostate, colon, and lung cancer [2–6]. More recent analyses of these data indicate that the association of IGF-1 and cancer is modest [7]. Altered IGF-1R levels in tumor versus normal tissue have been observed [8–15], with IGF-1R overexpression occurring in the earlier stages followed by IGF-1R downregulation in the later, dedifferentiated stages of breast [16–19] and prostate [20,21] cancer. Consistent with these observations, IGFBP-3 may be a negative risk factor for lung cancer [6,22]. Accordingly, the use of multiple strategies to block activation of the IGF-1R have been applied toward reducing tumor growth in vitro and in vivo [23].

The IGFBPs represent a class of IGF-1/2 antagonists that act by binding their ligands with high affinity and blocking their access to the IGF-1R [23]. Accordingly, the IGFBPs or IGFBP-mimetics may serve as lead compounds for development of small molecule IGF antagonists. Using high-throughput phage display to screen for IGF-1 interacting peptides, Deshayes et al. [24] identified a cyclic hexadecapeptide, IGF-F1-1, that specifically binds to IGF-1 with μM affinity. NMR analysis of the IGF-F1-1:IGF-1 complex revealed that the hydrophobic surface of IGF-F1-1 comprised of residues Phe-4, Val-7, Leu-10 and Met-14, contributes ~75% of the IGF-1 binding interface [25]. A similar hydrophobic region on IGF-1, including Leu-5, Ala-13, Phe-16, Val-17 and Leu-54 contributes ~55% of the IGF-F1-1 binding site. The importance of IGF-F1-1 residues, Phe-4, Ser-6, Val-7, Leu-10, Arg-11 and Met-14 has been confirmed by a shotgun alanine scanning phage display technique [25,26].

Following IGFBP-binding, IGF-1 (and IGF-2) are sequestered from the IGF-1R, resulting in the natural antagonism of IGF-1R function. As such, the IGFBPs are candidate therapeutics with applications in diseases where IGF-1R signaling exacerbates clinical outcomes. Thus, any information regarding IGF-1:IGFBP binding or its disruption, may provide important insight into the design of more effective IGF-1 inhibitory drugs. Given that IGF-F1-1 interacts with the IGFBP-binding domain on IGF-1, additional studies on the biologic utility of IGF-F1-1 in blocking IGF-1 action may yield additional information regarding the IGF-1:IGFBP interaction. In this study we examined the efficacy of IGF-F1-1 in inhibiting IGF-1 action. To this end, our goal was to establish whether blockade of IGF-1 residues known to interact with IGF-F1-1 is sufficient to disrupt IGF-1 binding to the IGF-1R and downstream signaling.

2. Materials and methods

2.1. Materials

Recombinant human IGF-1 was kindly provided by Genentech, Inc. (South San Francisco, CA) or Tercica, Inc. (Brisbane, CA). IGFBP-2 was prepared as previously described [27]. The peptide, IGF-F1-1 (RNCFESVAALRRCMYG-NH_2), was synthesized by SynPep Corp. (Dublin, CA) or kindly provided by Dr. Sachdev Sidhu (Genentech, Inc). The HPLC column (Discovery® BIO Wide Bore C_{18}, 25 cm × 4.6 mm, 5 μm) was obtained from Supelco (Bellefonte, PA). The MCF-7 cell line was obtained from the American Type Culture Collection (ATCC; Manassas, VA). The somatostatin analogue, octreotide (SMS 201-995) was a gift from Bristol-Myers Squibb (New York, NY). The IGF-1R tyrosine kinase inhibitor, NVP-AEW541, was a gift from Dr. Francesco Hofmann (Novartis, Basel, Switzerland). The PI-3 kinase inhibitor, wortmannin was obtained from Calbiochem (San Diego, CA). Anti-pAkt (S473) and anti-Akt polyclonal antibodies were obtained from Cell Signaling Technology (Danvers, MA). Anti-IGF-1Rβ subunit polyclonal antibody was obtained from Santa Cruz (Santa Cruz, CA). Recombinant human IGFBP-3 (N109D) [28], anti-phosphotyrosine monoclonal antibody 4G10® and anti-IGFBP-2 polyclonal antibody were obtained from Upstate (Charlottesville, VA). All secondary antibodies were obtained from Chemicon (Temecula, CA). All other materials were of reagent grade or higher.

2.2. IGF-binding analysis of IGF-F1-1

^{125}I-IGF-1 (15–20,000 cpm, 10 nCi, 15 pM; Amersham Biosciences; Piscataway, NJ) IGFBP-2 or IGFBP-3 (2 ng) were combined with increasing amounts of IGF-F1-1. In some experiments the cyclic decapeptide, octreotide was added in place of IGF-F1-1 as a control. Binding assays were carried out at 4 °C for 16 h using polyethylene glycol precipitation to separate bound from free ligand as described [27]. For comparison, IGF-1 binding to IGFBP-2 and IGFBP-3 was also evaluated. Bound ^{125}I-IGF-1 was quantified in a Compugamma spectrometer (LKB-Wallac; Turku, Finland). Counts precipitated in the absence of IGFBP or IGF-F1-1 (non-specific binding) were subtracted to determine specific binding. IC_{50} and Hill slope values were calculated using the equation $B = B_{min} + B_{max}/(1 + 10^{(\log IC_{50} - \log[ligand])}) \times$ Hill slope where B is the concentration of bound ligand, B_{min} the minimum binding observed and B_{max} is the maximal binding observed. Prism® v. 4 (GraphPad Software, Inc., San Diego, CA) was used to minimize the sum of the squares of the differences from the mean IC_{50} values for each concentration of IGF-1 to generate

best-fit curves for each sample set. Results were compared using a one-way analysis of variance. A Bonferroni post-test was performed on individual data sets if the $p < 0.05$ for the overall analysis. *t*-Tests (two-tailed, unpaired) in which individual Hill slopes were compared to each other as well as to the value of −1.0, which is indicative of a simple bimolecular ligand–receptor interaction, were also performed.

2.3. Cell culture

MCF-7 cells were maintained in RPMI medium pH 7.4 supplemented with L-glutamine (0.3 mg/ml), $NaHCO_3$ (2 mg/ml), and 10% FBS and penicillin (100 U/ml)–streptomycin (100 μg/ml). Cells were incubated at 37 °C in an atmosphere of 95% O_2 and 5% CO_2 in a humidified incubator. Cell lines were not passaged more than 30 times following placement in culture.

2.4. ^{125}I-IGF-1 binding to MCF-7 cells

MCF-7 cells ($\sim 1.9 \times 10^6$) were plated in 12-well dishes and supplemented with growth medium. After 24 h the growth medium was removed and replaced with serum free medium (SFM) for 24 h. At this time cells were incubated with ^{125}I-IGF-1 (15–20,000 cpm, 10 nCi, 15 pM) ± various concentrations of IGF-F1-1 (0.1–100 μM) or octreotide (1–10 μM) ± 500 nM unlabeled IGF-1. Treatment components were combined in HMS ± buffer (25 mM HEPES, 104 mM NaCl, 5 mM $MgCl_2$, 0.01% soybean trypsin inhibitor, 0.2% BSA pH 7.4) and pre-incubated at 37 °C, with nutating, for 1 h and then added to the cells for 30 min at 23 °C with constant nutating. Cells were washed once with HMS ± buffer followed by addition of 2N NaOH to dissolve the cells. The extracts so generated were collected into tubes and bound ^{125}I-IGF-1 quantified in a Compugamma spectrometer (LKB-Wallac; Turku, Finland). IC_{50} and Hill slope values were calculated as described above.

2.5. IGF-1Rβ subunit phosphorylation and Akt phosphorylation in MCF-7 cells

For IGF-1R phosphorylation experiments, MCF-7 cells ($\sim 5 \times 10^6$) were plated on 10 cm dishes and supplemented with growth medium for 24 h. Cells were serum-starved and treated with the indicated compounds as described in the figure legends. Equal amounts of whole cell lysate protein (1–2 mg) were diluted with STE (100 mM NaCl, 100 mM Tris pH 7.4, and 1 mM EDTA pH 7.4) to a final concentration of 0.1% Triton X-100 and incubated with protein A conjugated agarose (40 μl of a 1:1 slurry) plus anti-IGF-1Rβ subunit polyclonal antibody (15 μl) for 16 h at 4 °C. The beads were then centrifuged at 3000 rpm for 15 min at 4 °C and washed three times with lysis buffer containing 0.1% Triton X-100 and eluted with SDS-sample buffer containing dithiothreitol (100 mM). Proteins were resolved on a 10% SDS-polyacrylamide gel and transferred to a nitrocellulose membrane and immunoblotted with anti-phosphotyrosine (anti-pY) 4G10® monoclonal antibody (1:1000 dilution). The blot was developed with goat anti-mouse-horse radish peroxidase (HRP) IgG (1:4000 dilution) and the ECL reagent. The blot was then stripped with Re-blot mild stripping reagent and reprobed with anti-IGF-1Rβ subunit polyclonal antibody (1:500 dilution). For the analysis of Akt phosphorylation $\sim 1 \times 10^6$ MCF-7 cells were plated in 60 mm dishes and prepared for experiments as detailed above. Blots were probed with anti-pAkt (S473) antibodies and reprobed with anti-Akt polyclonal antibody (1:1000 dilution). When possible, densitometry was performed on the bands to assess differences between intensities using the program NIH Image® v. 1.61.

2.6. Cell cycle analysis of MCF-7 cells

MCF-7 cells ($\sim 1 \times 10^6$) were plated in 60 mm dishes and serum starved as described. Following treatment, the cells were harvested by trypsinization, washed with PBS, pH 7.4 and resuspended in 0.5 ml PBS in new tubes. Cells were fixed in ice-cold ethanol (70% final) for 16 h at 4 °C, washed twice with PBS and stained with 0.5–1 ml of propidium iodide staining cocktail (30 μM propidium iodide, 0.1 M EDTA, 0.1 mg/ml (7.5 U/ml) RNAse, and 0.1% Triton X-100 in PBS) for 15 min, at 37 °C in the dark. Samples were analyzed in the Hollings Cancer Center Flow Cytometry Facility using CellQuest Pro software optimized for cell cycle analysis using doublet discrimination on a FACSCalibur™ analytical flow cytometer (Becton Dickinson; San Jose, CA). Cell cycle analysis was performed on ModFit LT modeling software. Results were compared using a one-way analysis of variance within Prism® v. 4. A Bonferroni post-test was performed on individual data sets if the $p < 0.05$ for the overall analysis.

2.7. [^{3}H]Thymidine incorporation in MCF-7 cells

MCF-7 cells (5×10^4) were plated in 48-well dishes and serum-starved. At this time cells were treated for 21 h as indicated in the figure legend. Incubations were terminated by aspirating the medium and washing the cells with PBS. [^{3}H]thymidine (1 μCi/ml, 200 μl) in SFM containing 0.5% BSA was added to each well and incubated for 4 h at 37 °C in an atmosphere of 95% O_2 and 5% CO_2 in a humidified incubator. Medium was removed and the cells were washed three times with PBS. Cold TCA (12.5%, 0.5 ml) was then added to each well. After 15 min at 4 °C the TCA was removed and replaced with fresh TCA. This was repeated two more times after which the TCA was removed and 0.2N NaOH (250 μl) was added. After 25 min at 23 °C with constant mixing, 200 μl aliquots of the NaOH solution was removed from each well, transferred to a scintillation vial and combined with 5 ml EcoLume scintillation fluid (MP Biomedicals, Irvine, CA) for analysis in a 1900TR Liquid Scintillation Analyzer (Perkin-Elmer; Wellesley, MA). Results were compared using one-way analysis of variance (Prism® v. 4). A Bonferroni post-test was performed on individual data sets if $p < 0.05$ for the overall analysis.

3. Results

3.1. IGFBP competition binding studies

Competition binding studies were carried out using ^{125}I-IGF-1 (15–20,000 cpm, 10 nCi, 15 pM) plus IGFBP-2 or IGFBP-3 (2 ng) and increasing amounts of IGF-F1-1 (0.1 nM–2.6 μM

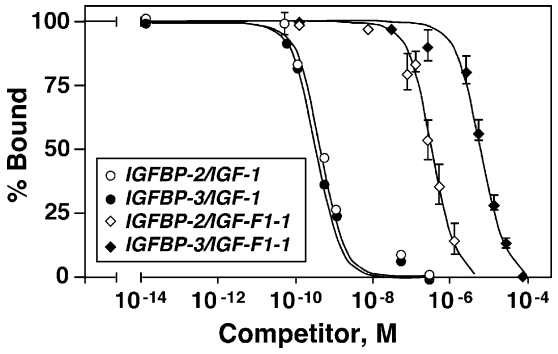

Fig. 1 – Competition binding analyses of IGF-F1-1 vs. IGFBP-2 or IGFBP-3 for IGF-1 binding. Solution phase-binding studies were conducted to evaluate the IC_{50} for IGF-F1-1 inhibition of IGF-1 binding to IGFBP-2 and IGFBP-3. Constant concentrations of ^{125}I-IGF-1 and IGFBP-2/IGFBP-3 were incubated with increasing doses of IGF-F1-1. Binding analyses were also performed with each IGFBP using unlabeled IGF-1 as competitor. Data points shown are the average values of three independent experiments performed in triplicate. Binding curves were generated as described under Section 2.

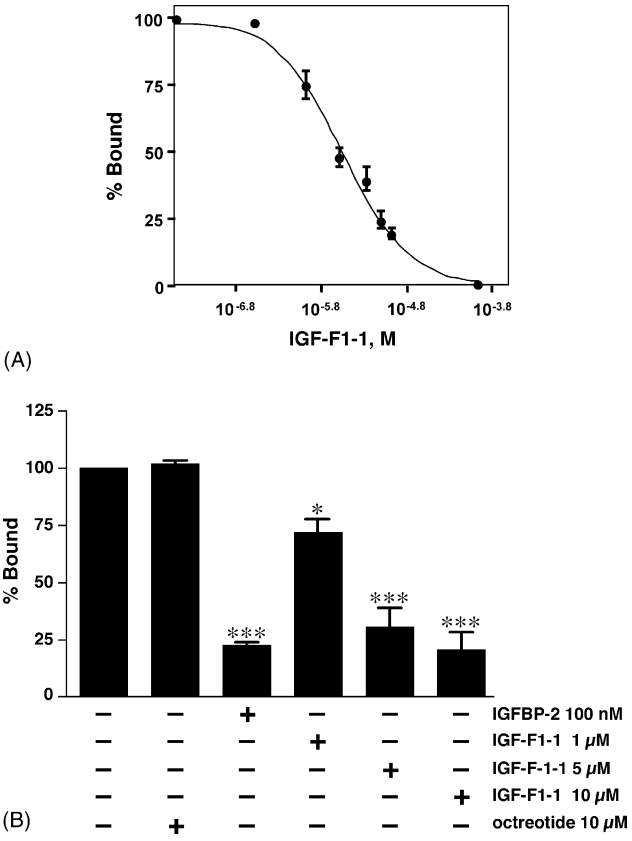

Fig. 2 – Inhibition of IGF-1 binding to MCF-7 cell IGF-1Rs. Competition binding analysis was performed on MCF-7 cells to determine the effect of IGF-F1-1 on cell surface binding of ^{125}I-IGF-1. (A) A full range of IGF-F1-1 doses on ^{125}I-IGF-1 binding was examined. Data points shown are the average values of three independent experiments performed in triplicate. Binding curves were generated as described under Section 2. (B) Addition of IGF-F1-1 as well as IGFBP-2 significantly inhibited ^{125}I-IGF-1 binding to the cells. p values represent comparisons made to total binding (bar 1). Octreotide had no effect on ^{125}I-IGF-1 binding. $^{*}p < 0.05$, $^{***}p < 0.001$.

for IGFBP-2 experiments; 0.1 nM–66.7 μM for IGFBP-3 experiments). The IC_{50} for IGF-F1-1 competition with IGFBP-2 was 331 ± 36.4 nM (Fig. 1). The IC_{50} for IGF-F1-1 competition with IGFBP-3 was 6.8 ± 0.88 μM (Fig. 1). Hill slopes for both the IGFBP-2 and IGFBP-3 curves were not significantly different from each other ($p > 0.05$, t-test) nor were they significantly different from −1.0 ($p > 0.05$, t-test). Addition of octreotide (2.6 μM (IGFBP-2) or 66.7 μM (IGFBP-3)) in place of IGF-F1-1 had no effect on IGF-1 binding to either binding protein (data not shown).

For comparison, competition binding analyses were performed using unlabeled IGF-1 as the competing ligand (Fig. 1). The IC_{50} for IGF-1 binding to IGFBP-2 was 0.42 ± 0.058 nM and for IGFBP-3 was 0.35 ± 0.05 nM, indicating IGF-1 had a 1.2-fold higher affinity for IGFBP-3 than for IGFBP-2. As observed with IGF-F1-1, Hill slopes were not significantly different from each other ($p > 0.05$, t-test). In summary, IGF-F1-1 competed with IGFBP-2 for IGF-1 binding with low affinity (331 ± 36.4 nM) compared to the affinity of IGF-1 for IGFBP-2 (0.42 ± 0.058 nM). An even more dramatic difference in affinities was observed with IGFBP-3.

3.2. *Inhibition of IGF-1 binding to MCF-7 cells by IGF-F1-1*

To determine whether IGF-F1-1 binding to IGF-1 could also block IGF-1 binding to the IGF-1R, competition binding studies were carried out using MCF-7 cells. Increasing doses of IGF-F1-1 (0.1–100 μM) were pre-incubated with ^{125}I-IGF-1 (15–20,000 cpm, 10 nCi, 15 pM) for 1 h prior to addition to MCF-7 cells for a 30 min binding assay. IGF-F1-1 inhibited the cell surface association of ^{125}I-IGF-1 in a dose-dependent manner (Fig. 2A). The IC_{50} for inhibition of MCF-7 cell binding was 2.8 ± 0.3 μM. Addition of 1 μM and greater concentrations of IGF-F1-1 caused significant inhibition of ^{125}I-IGF-1 binding to MCF-7 cells compared with total binding ($p < 0.05$ for 1 μM, $p < 0.001$ for 5 and 10 μM). IGFBP-2 (100 nM) inhibited ^{125}I-IGF-1 binding by 75% while addition of octreotide (10 μM) had no effect on ^{125}I-IGF-1 binding (Fig. 2B). ANOVA analysis showed that IGFBP-2 significantly inhibited ^{125}I-IGF-1 binding compared to ^{125}I-IGF-1 alone ($p < 0.001$), while cell binding observed in the presence of octreotide was not significantly different from total binding achieved in the absence of competing ligand ($p > 0.05$).

3.3. *IGF-1R phosphorylation*

The effects of either IGF-1 or IGF-F1-1 alone or combined on IGF-1Rβ-subunit tyrosine phosphorylation were examined using in MCF-7 cells and an immunoprecipitation:immunoblot (IP:IB) protocol (Fig. 3). IGF-1 stimulated IGF-1R phosphorylation was detectable within 5 min of exposure to MCF-7 cells. IGF-1 induced IGF-1R phosphorylation was inhibited by the addition of the IGF-1R tyrosine kinase inhibitor, NVP-AEW541

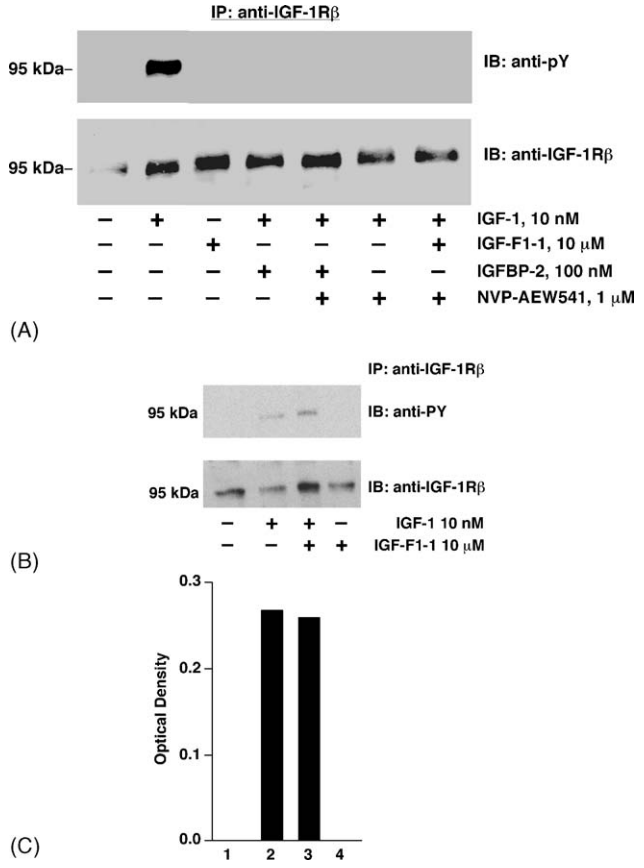

Fig. 3 – Effect of IGFBP-2 and NVP-AEW541 on IGF-1-induced IGF-1R tyrosine phosphorylation in MCF-7 cells. MCF-7 cells were treated with the indicated reagents for 5 min. Immunoprecipitation (IP) followed by immunoblot (IB) of MCF-7 whole cell extracts (WCE) was completed. (A) IGF-1 stimulated IGF-1R phosphorylation, which was inhibited by NVP-AEW541 and IGFBP-2 (lanes 4–7). IGF-F1-1 had no detectable effect on IGF-1R phosphorylation. (B) Co-addition of IGF-1 and IGF-F1-1 did not significantly alter IGF-1R tyrosine phosphorylation compared to that stimulated by IGF-1 alone. (C) Densitometric analysis of gel shown in (B). Similar results were obtained in three separate experiments.

[29] and by IGFBP-2 (Fig. 3A). IGF-F1-1 addition had no detectable effect on IGF-1Rβ-subunit phosphorylation when added alone or in the presence of IGF-1 (Fig. 3B).

3.4. *Analysis of Akt phosphorylation*

IGF-1R signaling via PI-3 K leads to Akt activation and downstream growth and anti-apoptotic signals. IGF-1 stimulated Akt phosphorylation in MCF-7 cells was inhibited by NVP-AEW541 and IGFBP-2 addition, but not by IGF-F1-1 (Fig. 4A and B). Rather, a slight increase in Akt phosphorylation over IGF-1 treatment alone was seen with the co-addition of IGF-1 and IGF-F1-1. Treatment of MCF-7 cells with IGF-F1-1 alone caused Akt phosphorylation (Fig. 4A and B) comparable to IGF-1 treatment. IGF-F1-1 stimulated Akt phosphorylation was inhibited by NVP-AEW541 or IGFBP-2 treatment, suggesting IGF-1R involvement in IGF-F1-1 stimulated Akt activation. IGF-F1-1 caused a dose-dependent stimulation of Akt phosphorylation while having no effect on Erk 1/2 phosphorylation (Fig. 4C). Octreotide had no effect on Akt phosphorylation (Fig. 4B).

3.5. *Cell cycle analysis*

To examine the biologic effects of IGF-F1-1 on MCF-7 cell function, cell cycle analysis was performed (Fig. 5). Growth of cells in SFM (control) yielded a low percentage of cells in S-phase ($4.45 \pm 0.86\%$) with the majority in G_1 ($91.15 \pm 2.16\%$). IGF-1 treatment significantly increased the percentage of cells in S-phase ($19.18 \pm 0.76\%$, $p < 0.001$), which coincided with a decrease in the number of cells in G_1 ($65.72 \pm 1.52\%$). Co-addition of IGFBP-2 and IGF-1 significantly reduced the number of cells in S-phase compared to IGF-1 treatment alone ($p < 0.05$). Co-addition of IGF-1 with IGF-F1-1 (5 or 10 μM)

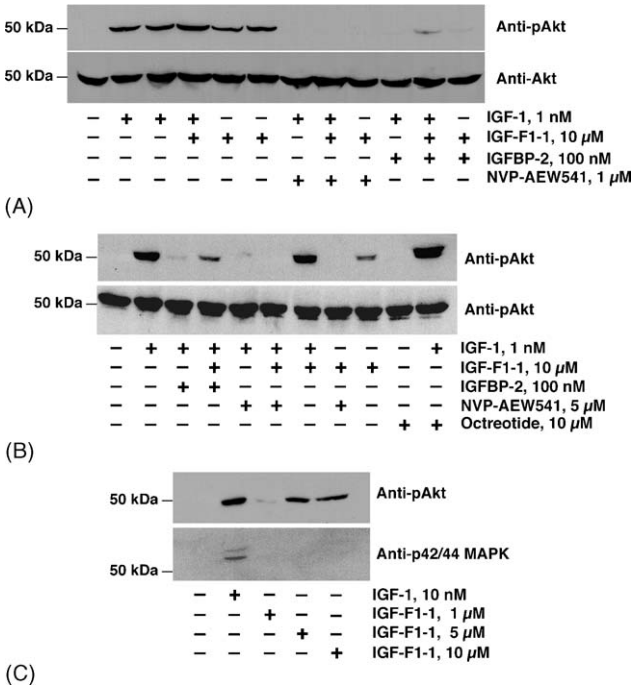

Fig. 4 – Dose dependent phosphorylation of Akt by IGF-F1-1 A/B, cells were treated with the indicated reagents for 15 min. WCEs were prepared and equal amounts of total protein was immunoblotted with anti-pAkt and anti-Akt antibodies. IGF-1 and IGF-F1-1 stimulated Akt phosphorylation was inhibited by NVP-AEW541 and IGFBP-2. IGF-1 and IGF-F1-1 stimulated phosphorylation was inhibited by NVP-AEW541 and IGFBP-2. The control cyclic peptide octreotide did not stimulate phosphorylation of Akt. C, Cells were treated with IGF-1 or IGF-F1-1 for 15 min. Equal amounts of total protein from WCEs was immunoblotted with anti-pAkt and anti-p44/42 MAPK antibodies. IGF-1 stimulated phosphorylation of Akt as well as Erk1 and Erk 2. A positive dose-response effect on Akt phosphorylation was observed with IGF-F1-1. Each blot shown is representative of at least three independent experiments.

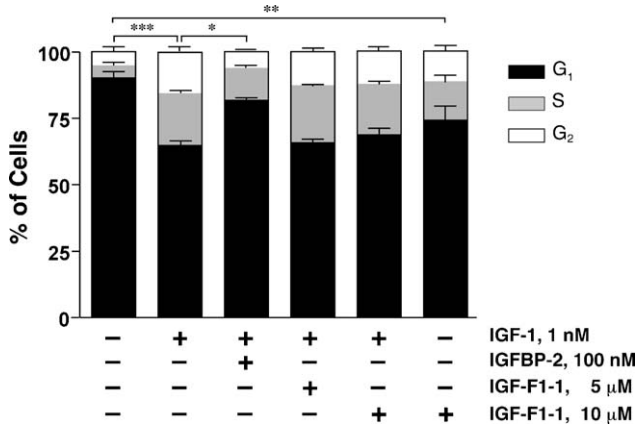

Fig. 5 – IGF-1 and IGF-F1-1 regulated MCF-7 cell cycle changes. IGF-1 promoted the transition of cells from G_1 to S-phase. This effect was inhibited by co-addition of IGFBP-2 but not by IGF-F1-1. A statistically significant increase in the number of cells transitioning from G_1 to S-phase was observed upon addition of IGF-F1-1. Bars represent the mean of three independent experiments performed in duplicate. Error bars indicate standard error from the mean. $^{*}p < 0.05$, $^{**}p < 0.01$, $^{***}p < 0.001$.

did not significantly change the cell cycle profile compared to IGF-1 treatment alone. However, IGF-F1-1 treatment alone significantly increased the percentage of cells in S-phase ($14.8 \pm$ S.E. 2.8%; $p < 0.01$) and decreased the percentage of cells in G_1 ($74.9 \pm$ S.E. 4.9%; $p < 0.01$) compared to control.

3.6. [^{3}H]thymidine incorporation in MCF-7 cells

To further verify that the effects of IGF-F1-1 on cell cycle changes reflected growth responses, IGF-F1-1 stimulated [^{3}H]thymidine incorporation was evaluated. IGF-1 stimulated an 11.8-fold increase in [^{3}H]thymidine incorporation compared to control cells exposed to SFM alone ($p < 0.001$; Fig. 6). IGFBP-2 (100 nM) significantly reduced IGF-1 stimulated [^{3}H]thymidine incorporation (1.9-fold, $p < 0.001$) (Fig. 6). Wortmannin and NVP-AEW541 each caused a pronounced inhibition of IGF-1 induced [^{3}H]thymidine incorporation (Fig. 6). IGF-F1-1 stimulated a 7.6-fold increase in [^{3}H]thymidine incorporation ($p < 0.001$), which was reduced to control levels by the addition of either IGFBP-2, wortmannin or NVP-AEW541. Addition of IGF-F1-1 in the presence of IGF-1 had no appreciable effect on [^{3}H]thymidine incorporation over IGF-1 treatment alone ($p > 0.05$, ns). However, the level of inhibition obtained with IGFBP-2 was reduced when IGF-1 was added with IGF-F1-1, compared to that observed for IGFBP-2 inhibition of IGF-1. This difference reflected the increased activity accompanying IGF-F1-1 treatment. A more pronounced inhibition of [^{3}H]thymidine incorporation was obtained when the combined actions of IGF-1 and IGF-F1-1 were inhibited with wortmannin or NVP-AEW541 treatment.

4. Discussion

In standard competition binding assays IGF-F1-1 competed with IGFBP-3 (IC_{50} 6.8 ± 0.88 μM) and IGFBP-2 (IC_{50} 331 ± 36.4 nM) for IGF-1 binding. This represents a 20.5-fold lower IC_{50} for IGFBP-2 compared to IGFBP-3. The value obtained for IGFBP-3 was ~2.3-fold lower than what was reported for IGF-F1-1 competing with IGFBP-3 in phage ELISA assays with IGFBP-3 (IC_{50} 2.9 μM) and IGFBP-1 (IC_{50} 1.4 μM) competing with IGF-F1-1 for IGF-1 [24]. The Hill slopes for IGFBP-2 and IGFBP-3 were not significantly different from each other nor from a value of −1.0, suggesting the existence of a simple, bimolecular or one-site model for the binding of IGF-1 to IGFBP-2 and IGFBP-3. Importantly, these data further suggest the potential for a differential binding interaction with respect to the manner in which IGFBP-2 and IGFBP-3 contact IGF-1. This suggests that IGF-F1-1 possesses structural characteristics that are more comparable to IGFBP-2 than for IGFBP-3. Recent NMR studies on bovine IGFBP-2 bound to IGF-1 or IGF-2 revealed an interaction between the C-terminus of IGFBP-2 and IGF-1 residues Leu-14, Gln-15, Gly-22-Phe-25; all of which are important in IGF-1R receptor binding [30]. Mutagenesis studies have revealed the importance of residues within the C-terminus of IGFBP-2 in IGF

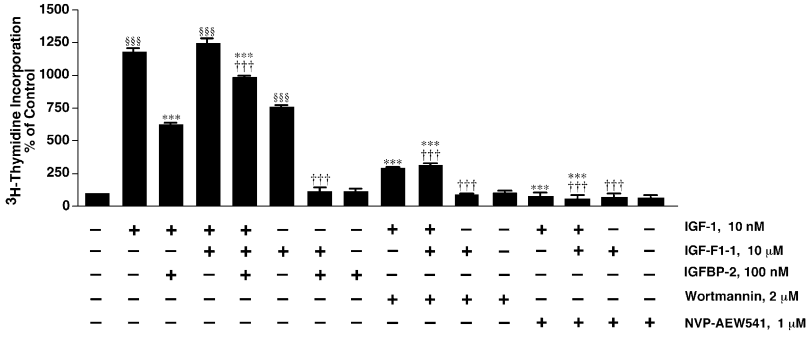

Fig. 6 – IGF-1 and IGF-F1-1 stimulated [^{3}H]thymidine incorporation in MCF-7 cells. Serum-starved MCF-7 cells were treated as indicated for 21 h. [^{3}H]thymidine incorporation was then allowed to proceed for 4 h, followed by processing of the cells for analysis. IGF-1 and IGF-F1-1 each stimulated a significant increase in [^{3}H]thymidine incorporation compared to control cells, which was inhibited, in each case, by IGFBP-2. Bars represent mean values of three independent experiments performed in triplicate. Error bars represent standard error of the mean. $^{§§§}p < 0.001$ compared to control, $^{†††}p < 0.001$ compared to IGF-F1-1, $^{***}p < 0.001$ compared to IGF-1.

binding [27,31–35] while N-terminal residues have been implicated in IGFBP-3 binding [28,35]. Taken together, these observations imply that these two IGFBPs bind IGF-1 by somewhat different mechanisms. The higher affinity IGF-1 has for IGFBP-3 compared to IGFBP-2, may, in part, contribute to the differences in affinity observed with IGF-F1-1 in our binding assays. The affinities reported here are in agreement with those observed by Deshayes et al. [24].

To examine whether the IGF-F1-1:IGF-1 interaction impacts the ability of IGF-1 to bind to and engage the IGF-1R, binding studies with MCF-7 cells were carried out. IGF-F1-1 inhibited ^{125}I-IGF-1 binding to MCF-7 cells in a dose-dependent manner with an $IC_{50} = 2.8 \pm 0.3$ μM and a Hill slope -1.1 ± 0.62. These data were in agreement with those reported by Deshayes et al. who observed an $IC_{50} = 5.1$ μM for binding to the IGF-1R [24].

We did not observe IGF-F1-1 inhibition of downstream IGF-1 signaling. Essentially no change was observed in IGF-1 stimulated IGF-1R phosphorylation, Akt phosphorylation, cell cycle profile, or [^{3}H]thymidine incorporation in MCF-7 cells upon co-addition of IGF-1 and IGF-F1-1. Based on the observed inhibition of IGF-1 binding to the IGF-1R and the inhibition of IGF-1 binding to IGFBP-2 and IGFBP-3, blockade of IGF-1 induced signaling events was expected. We used 15 pM ^{125}I-IGF-1 in our MCF-7 cell binding studies, whereas Deshayes et al. [24] used 2 nM ^{125}I-IGF-1. Given the inability of IGF-F1-1 to significantly inhibit IGF-1-induced IGF-1R phosphorylation, Akt phosphorylation, S-phase transition, and [^{3}H]thymidine incorporation, we conclude that IGF-F1-1 has a very low potency for inhibiting IGF-1 binding to the IGF-1R.

Paradoxical effects were observed upon addition of IGF-F1-1 alone to MCF-7 cells. IGF-F1-1 stimulated Akt phosphorylation, S-phase entry, and [^{3}H]thymidine incorporation. On this basis, it is capable of eliciting mitogenic effects. However, IGF-F1-1 did not stimulate Erk activation. The effect of IGF-F1-1 on Akt phosphorylation was inhibited by IGFBP-2 and the IGF-1R tyrosine kinase inhibitor, NVP-AEW541. Similarly, induction of [^{3}H]thymidine incorporation in MCF-7 cells by IGF-F1-1 was blocked by addition IGFBP-2, NVP-AEW541, and the PI-3K inhibitor, wortmannin. These results suggest that the effects of IGF-F1-1 are IGF-1, IGF-1R, and PI-3K dependent. Although, Akt phosphorylation and [^{3}H]thymidine incorporation were blocked by NVP-AEW541, IGF-F1-1 stimulated IGF-1R phosphorylation was not detected. The simplest explanation for this is that the low signal intensity achieved in anti-phosphotyrosine immunoblot analysis was likely too weak to enable detection of IGF-F1-1-dependent IGF-1R phosphorylation. Along these lines, it is also possible that the IP:IB approach used was ineffective at identifying select populations of phosphotyrosines within the IGF-1R β-subunit, either due to antibody specificity for phosphotyrosines in select environments or the presence of interacting proteins bound to these phosphotyrosines following IGF-F1-1 treatment, thereby blocking antibody access. Related to this, phosphorylation of tyrosines 1250 and 1251 are essential for Erk activity, but unnecessary for PI3K/Akt activation [36]. If our assay was more effective at reporting the phosphorylation of these tyrosines, it may not accurately reflect signaling to Akt.

Significantly, the observation that IGFBP-2 blocked the effects of IGF-F1-1 suggests that it may be acting in an IGF-dependent manner. Binding of IGFBP-IGF complexes to the ECM creates a reservoir for IGF-1 near IGF-1Rs in the cell membrane [37–40]. The interaction of IGFBPs with the ECM reduces their affinity for the IGFs thereby facilitating IGF release for subsequent IGF-1R activation. Several studies have demonstrated association of IGFBP-3, IGFBP-5, IGF-1, and IGF-2 as well as complexes of IGFBPs and IGFs with ECM proteins in MCF-7 cell cultures [41]. On this basis, we propose that the low affinity binding of IGF-1 by ECM associated IGFBPs, may facilitate IGF-F1-1 induced dissociation of IGF-1. This provides an explanation for the observed inhibition of IGF-F1-1 induced Akt phosphorylation and [^{3}H]thymidine incorporation by exogenously added IGFBP-2. Alternatively, IGF-F1-1 may itself bind to IGFBP-2. In this case, inhibition of IGF-F1-1 induced Akt phosphorylation and [^{3}H]thymidine incorporation may be due to a direct interaction/inhibition of IGF-F1-1 with IGFBP-2. This would be consistent with the direct stimulation of the IGF-1R or an alternative receptor tyrosine kinase by IGF-F1-1.

An alternative explanation for the paradoxical effects observed is that IGF-F1-1 via IGF-1 release is stimulating another pathway. Crosstalk between the IGF-1R and the G-protein coupled chemokine receptors CXCR4 [42] and CCR5 [43] have recently been observed. Akekawatchai and colleagues [42] demonstrated a direct interaction between CXCR4 and the IGF-1R, resulting in IGF-1 mediated cell migration in MDA-MB-231 cells that was partially inhibited by CXCR4 RNAi or pertussis toxin. IGF-1R activation also causes CCR5 activation via induction and autocrine action of RANTES [43]. Finally, the IGF-1R also transactivates EGFR1 through proteinase-dependent release of heparin-binding EGF [44] and EGFR-2 (HER-2) via physical association [45]. Thus, CXCR4, CCR5, EGFR-1 and HER-2 are examples of receptors known to engage in crosstalk with the IGF-1R and represent alternative pathways that may be affected either directly or indirectly by IGF-F1-1.

In summary, we have examined the biologic actions of the phage display peptide, IGF-F1-1 using in vitro and cell-based assays. We confirmed previous reports demonstrating that IGF-F1-1 competes with IGFBP-3 for binding to IGF-1 and extended them to IGFBP-2 binding. Our results indicated different inhibition profiles for IGFBP-2 and IGFBP-3 consistent with the notion that the interactions of these binding proteins with IGF-1 differ. We further showed that treatment of MCF-7 cells with IGF-F1-1 results in Akt phosphorylation, [^{3}H]thymidine incorporation and S-phase transition. All of these effects could be abrogated by the addition of IGFBP-2 or NVP-AEW541, suggesting that IGF-F1-1 acts as an indirect agonist, releasing IGFBP-bound IGF-1.

Acknowledgments

We thank Genentech, Inc. and Tercica, Inc. for generously providing recombinant human IGF-1. Dr. Sachdev Sidhu (Department of Protein Engineering, Genentech, Inc.) also provided IGF-F1-1 peptide and insight concerning its structure and mechanisms of action. We also thank Dr. Erika Büllesbach, MUSC, for advice on the oxidation of the IGF-F1-1 peptide used in these experiments and members of the Rosenzweig laboratory for helpful discussions. We acknowledge the Hollings Cancer Center Flow Cytometry and the

MUSC Mass Spectrometry Facilities for technical advice. This research was supported by National Institutes of Health grant CA78887, Department of Defense grant N6311601MD10004 and a Hollings Cancer Center/Medical University of South Carolina Department of Defense grant ''Translational Research on Cancer Control and Related Therapy'' (Subcontract GC-3319-05-4498CM). Stephanie A. Robinson was supported by dissertation research award DISS0201947 from the Susan G. Komen Breast Cancer Foundation.

Appendix A. Supplementary data

Supplementary data associated with this article can be found, in the online version, at doi:10.1016/j.bcp.2006.03.025.

REFERENCES

[1] Sell C, Rubini M, Rubin R, Liu JP, Efstratiadis A, Baserga R. Simian virus 40 large tumor antigen is unable to transform mouse embryonic fibroblasts lacking type 1 insulin-like growth factor receptor. Proc Natl Acad Sci USA 1993;90(23):11217–21.
[2] Hankinson SE, Willett WC, Colditz GA, Hunter DJ, Michaud DS, Deroo B, et al. Circulating concentrations of insulin-like growth factor-I and risk of breast cancer. Lancet 1998;351(9113):1393–6.
[3] Chan JM, Stampfer MJ, Giovannucci E, Gann PH, Ma J, Wilkinson P, et al. Plasma insulin-like growth factor-I and prostate cancer risk: a prospective study. Science 1998;279(5350):563–6.
[4] Ma J, Pollak MN, Giovannucci E, Chan JM, Tao Y, Hennekens CH, et al. Prospective study of colorectal cancer risk in men and plasma levels of insulin-like growth factor (IGF)-I and IGF-binding protein-3. J Natl Cancer Inst 1999;91(7):620–5.
[5] Wolk A, Mantzoros CS, Andersson SO, Bergstrom R, Signorello LB, Lagiou P, et al. Insulin-like growth factor 1 and prostate cancer risk: a population-based, case-control study. J Natl Cancer Inst 1998;90(12):911–5.
[6] Yu H, Spitz MR, Mistry J, Gu J, Hong WK, Wu X. Plasma levels of insulin-like growth factor-I and lung cancer risk: a case-control analysis. J Natl Cancer Inst 1999;91(2):151–6.
[7] Renehan AG, Zwahlen M, Minder C, O'Dwyer ST, Shalet SM, Egger M. Insulin-like growth factor (IGF)-I, IGF binding protein-3, and cancer risk: systematic review and meta-regression analysis. Lancet 2004;363(9418):1346–53.
[8] Khandwala HM, McCutcheon IE, Flyvbjerg A, Friend KE. The effects of insulin-like growth factors on tumorigenesis and neoplastic growth. Endocr Rev 2000;21(3):215–44.
[9] Quinn KA, Treston AM, Unsworth EJ, Miller MJ, Vos M, Grimley C, et al. Insulin-like growth factor expression in human cancer cell lines. J Biol Chem 1996;271(19):11477–83.
[10] Steller MA, Delgado CH, Bartels CJ, Woodworth CD, Zou Z. Overexpression of the insulin-like growth factor-1 receptor and autocrine stimulation in human cervical cancer cells. Cancer Res 1996;56(8):1761–5.
[11] Resnik JL, Reichart DB, Huey K, Webster NJ, Seely BL. Elevated insulin-like growth factor I receptor autophosphorylation and kinase activity in human breast cancer. Cancer Res 1998;58(6):1159–64.
[12] Xie Y, Skytting B, Nilsson G, Brodin B, Larsson O. Expression of insulin-like growth factor-1 receptor in synovial sarcoma: association with an aggressive phenotype. Cancer Res 1999;59(15):3588–91.
[13] Hakam A, Yeatman TJ, Lu L, Mora L, Marcet G, Nicosia SV, et al. Expression of insulin-like growth factor-1 receptor in human colorectal cancer. Hum Pathol 1999;30(10):1128–33.
[14] Krueckl SL, Sikes RA, Edlund NM, Bell RH, Hurtado-Coll A, Fazli L, et al. Increased insulin-like growth factor I receptor expression and signaling are components of androgen-independent progression in a lineage-derived prostate cancer progression model. Cancer Res 2004;64(23):8620–9.
[15] Weber MM, Fottner C, Liu SB, Jung MC, Engelhardt D, Baretton GB. Overexpression of the insulin-like growth factor I receptor in human colon carcinomas. Cancer 2002;95(10):2086–95.
[16] Schnarr B, Strunz K, Ohsam J, Benner A, Wacker J, Mayer D. Down-regulation of insulin-like growth factor-I receptor and insulin receptor substrate-1 expression in advanced human breast cancer. Int J Cancer 2000;89(6):506–13.
[17] Happerfield LC, Miles DW, Barnes DM, Thomsen LL, Smith P, Hanby A. The localization of the insulin-like growth factor receptor 1 (IGFR-1) in benign and malignant breast tissue. J Pathol 1997;183(4):412–7.
[18] Bartucci M, Morelli C, Mauro L, Ando S, Surmacz E. Differential insulin-like growth factor I receptor signaling and function in estrogen receptor (ER)-positive MCF-7 and ER-negative MDA-MB-231 breast cancer cells. Cancer Res 2001;61(18):6747–54.
[19] Papa V, Gliozzo B, Clark GM, McGuire WL, Moore D, Fujita-Yamaguchi Y, et al. Insulin-like growth factor-I receptors are overexpressed and predict a low risk in human breast cancer. Cancer Res 1993;53(16):3736–40.
[20] Tennant MK, Thrasher JB, Twomey PA, Drivdahl RH, Birnbaum RS, Plymate SR. Protein and messenger ribonucleic acid (mRNA) for the type 1 insulin-like growth factor (IGF) receptor is decreased and IGF-II mRNA is increased in human prostate carcinoma compared to benign prostate epithelium. J Clin Endocrinol Metab 1996;81(10):3774–82.
[21] Chott A, Sun Z, Morganstern D, Pan J, Li T, Susani M, et al. Tyrosine kinases expressed in vivo by human prostate cancer bone marrow metastases and loss of the type 1 insulin-like growth factor receptor. Am J Pathol 1999;155(4):1271–9.
[22] Yu H, Rohan T. Role of the insulin-like growth factor family in cancer development and progression. J Natl Cancer Inst 2000;92(18):1472–89.
[23] Rosenzweig SA. What's new in the IGF-binding proteins? Growth Horm IGF Res 2004;14(5):329–36.
[24] Deshayes K, Schaffer ML, Skelton NJ, Nakamura GR, Kadkhodayan S, Sidhu SS. Rapid identification of small binding motifs with high-throughput phage display: discovery of peptidic antagonists of IGF-1 function. Chem Biol 2002;9(4):495–505.
[25] Schaffer ML, Deshayes K, Nakamura G, Sidhu S, Skelton NJ. Complex with a phage display-derived peptide provides insight into the function of insulin-like growth factor I. Biochemistry 2003;42(31):9324–34.
[26] Weiss GA, Watanabe CK, Zhong A, Goddard A, Sidhu SS. Rapid mapping of protein functional epitopes by combinatorial alanine scanning. Proc Natl Acad Sci USA 2000;97(16):8950–4.
[27] Kibbey MM, Jameson MJ, Eaton EM, Rosenzweig SA. Insulin-like growth factor binding protein-2: contributions of the C-terminal domain to IGF-1 binding. Mol Pharmacol 2005.
[28] Firth SM, Ganeshprasad U, Baxter RC. Structural determinants of ligand and cell surface binding of insulin-like growth factor-binding protein-3. J Biol Chem 1998;273(5):2631–8.

[29] Garcia-Echeverria C, Pearson MA, Marti A, Meyer T, Mestan J, Zimmermann J, et al. In vivo antitumor activity of NVP-AEW541–A novel, potent, and selective inhibitor of the IGF-IR kinase. Cancer Cell 2004;5(3):231–9.
[30] Carrick FE, Hinds MG, McNeil KA, Wallace JC, Forbes BE, Norton RS. Interaction of insulin-like growth factor (IGF)-I and -II with IGF binding protein-2: mapping the binding surfaces by nuclear magnetic resonance. J Mol Endocrinol 2005;34(3):685–98.
[31] Horney MJ, Evangelista CA, Rosenzweig SA. Synthesis and characterization of insulin-like growth factor (IGF)-1 photoprobes selective for the IGF-binding proteins (IGFBPS). photoaffinity labeling of the IGF-binding domain on IGFBP-2. J Biol Chem 2001;276(4):2880–9.
[32] Mark S, Kubler B, Honing S, Oesterreicher S, John H, Braulke T, et al. Diversity of human insulin-like growth factor (IGF) binding protein-2 fragments in plasma: primary structure, IGF-binding properties, and disulfide bonding pattern. Biochemistry 2005;44(9):3644–52.
[33] Forbes BE, Turner D, Hodge SJ, McNeil KA, Forsberg G, Wallace JC. Localization of an insulin-like growth factor (IGF) binding site of bovine IGF binding protein-2 using disulfide mapping and deletion mutation analysis of the C-terminal domain. J Biol Chem 1998;273(8):4647–52.
[34] Ho PJ, Baxter RC. Characterization of truncated insulin-like growth factor-binding protein-2 in human milk. Endocrinology 1997;138(9):3811–8.
[35] Yan X, Forbes BE, McNeil KA, Baxter RC, Firth SM. Role of N- and C-terminal residues of insulin-like growth factor (IGF)-binding protein-3 in regulating IGF complex formation and receptor activation. J Biol Chem 2004;279(51):53232–40.
[36] Leahy M, Lyons A, Krause D, O'Connor R. Impaired Shc, Ras, and MAPK activation but normal Akt activation in FL5 12 cells expressing an insulin-like growth factor I receptor mutated at tyrosines 1250 and 1251. J Biol Chem 2004;279(18):18306–13.
[37] Conover CA, Ronk M, Lombana F, Powell DR. Structural and biological characterization of bovine insulin-like growth factor binding protein-3. Endocrinology 1990;127(6):2795–803.
[38] Busby Jr WH, Klapper DG, Clemmons DR. Purification of a 31,000-dalton insulin-like growth factor binding protein from human amniotic fluid. Isolation of two forms with different biologic actions. J Biol Chem 1988;263(28):14203–10.
[39] Andress DL, Birnbaum RS. Human osteoblast-derived insulin-like growth factor (IGF) binding protein-5 stimulates osteoblast mitogenesis and potentiates IGF action. J Biol Chem 1992;267(31):22467–72.
[40] Jones JI, Gockerman A, Busby Jr WH, Camacho-Hubner C, Clemmons DR. Extracellular matrix contains insulin-like growth factor binding protein-5: potentiation of the effects of IGF-I. J Cell Biol 1993;121(3):679–87.
[41] Kricker JA, Towne CL, Firth SM, Herington AC, Upton Z. Structural and functional evidence for the interaction of insulin-like growth factors (IGFs) and IGF binding proteins with vitronectin. Endocrinology 2003;144(7):2807–15.
[42] Akekawatchai C, Holland JD, Kochetkova M, Wallace JC, McColl SR. Transactivation of CXCR4 by the insulin-like growth factor-1 receptor (IGF-1R) in human MDA-MB-231 breast cancer epithelial cells. J Biol Chem 2005;280(48):39701–8.
[43] Mira E, Lacalle RA, Gonzalez MA, Gomez-Mouton C, Abad JL, Bernad A, et al. A role for chemokine receptor transactivation in growth factor signaling. EMBO Rep 2001;2(2):151–6.
[44] Roudabush FL, Pierce KL, Maudsley S, Khan KD, Luttrell LM. Transactivation of the EGF receptor mediates IGF-1-stimulated shc phosphorylation and ERK1/2 activation in COS-7 cells. J Biol Chem 2000;275(29):22583–9.
[45] Nahta R, Yuan LX, Zhang B, Kobayashi R, Esteva FJ. Insulin-like growth factor-i receptor/human epidermal growth factor receptor 2 heterodimerization contributes to trastuzumab resistance of breast cancer cells. Cancer Res 2005;65(23):11118–2.